

Adsorption and retarded diffusion of Eu^{III} -EDTA -through hard clay rock.

Michael Descostes, Ingmar Pointeau, Jean Radwan, Jenna Poonoosamy,
Jean-Luc Lacour, Denis Menut, Thomas Vercouter, Romain V.H. Dagnelie

► **To cite this version:**

Michael Descostes, Ingmar Pointeau, Jean Radwan, Jenna Poonoosamy, Jean-Luc Lacour, et al..
Adsorption and retarded diffusion of Eu^{III} -EDTA -through hard clay rock.. Journal of Hydrology,
Elsevier, 2017, 544, pp.125-132. 10.1016/j.jhydrol.2016.11.014 . cea-02383154

HAL Id: cea-02383154

<https://hal-cea.archives-ouvertes.fr/cea-02383154>

Submitted on 27 Nov 2019

HAL is a multi-disciplinary open access archive for the deposit and dissemination of scientific research documents, whether they are published or not. The documents may come from teaching and research institutions in France or abroad, or from public or private research centers.

L'archive ouverte pluridisciplinaire **HAL**, est destinée au dépôt et à la diffusion de documents scientifiques de niveau recherche, publiés ou non, émanant des établissements d'enseignement et de recherche français ou étrangers, des laboratoires publics ou privés.

Supplementary material for

Adsorption and retarded diffusion of Eu^{III} -EDTA⁻ through hard clay rock.

Michael Descostes^a, Ingmar Pointeau^a, Jean Radwan^a, Jenna Poonoosamy^a,

Jean-Luc Lacour^b, Denis Menut^b, Thomas Vercoouter^b, Romain V. H. Dagnelie^{a,*}.

(a) DEN-Service d'Etude du Comportement des Radionucléides (SECR), CEA, Université Paris-Saclay, F-91191, Gif-sur-Yvette, France

(b) DEN-Service d'Etudes Analytiques et de Réactivité des Surfaces (SEARS), CEA, Université Paris-Saclay, F-91191, Gif-sur-Yvette, France

* Corresponding author. E-mail: romain.dagnelie@cea.fr

Content:

Table S1: Composition of synthetic porewater used for experiments	S2
Figure S1: Scheme of solid samples sliced for LIBS-micro probe characterization	S2
Figure S2: Adsorption kinetic of Eu-EDTA on clay rock sample	S3
Figure S3: Effect of adsorption kinetic on through-diffusion modelling	S4

Table S1. Synthetic poral water composition used for this study.

	Na ⁺	K ⁺	Ca ²⁺	Mg ²⁺	Sr ²⁺	Cl ⁻	ΣCO ₂	SO ₄ ²⁻	pH
C (10 ⁻³ moles L ⁻¹)	35.6	1.48	8.79	7.00	0.13	33.6	2.20	16.9	7.15

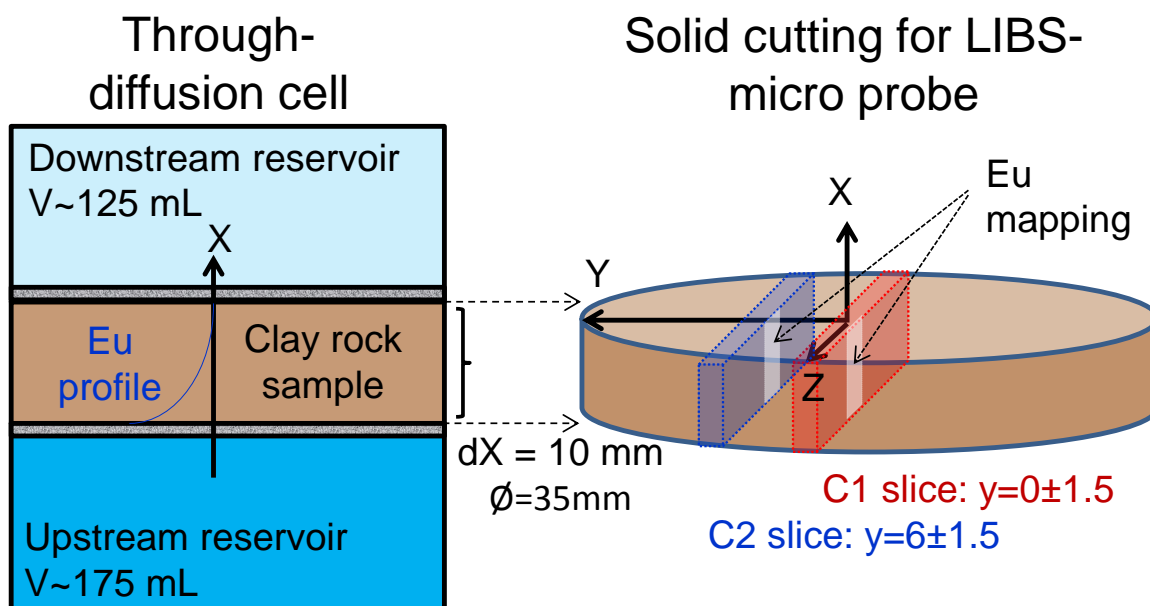


Figure S1. Scheme of solid samples sliced for LIBS-micro probe characterization.

(Left) Scheme of through-diffusion cell (diffusion gradient along X-axis).

(Right) Scheme of C1 and C2 solid samples sliced after diffusion.

A post-mortem characterization of the clay rock was performed after diffusion. To this aim, two rock samples were sliced. Eu mapping was measured by LIBS-micro probe technique. Several mapping were performed on center of C1 and C2 slices. Typical dimensions of mapping were $dX \times dZ \sim 10 \times 1$ mm² as shown in Fig. S1.

Adsorption kinetics of ¹⁵²Eu-EDTA and ¹⁴C-EDTA on COx clay rock

Adsorption kinetics for ¹⁵²Eu in presence of EDTA and ¹⁴C-EDTA was measured on COx clay rock up to 14 days. A rough estimation was performed assuming an exponential decay of concentration in solution. The kinetic rate was then extrapolated by linear regression on $\ln[(C(t)-C_{\infty})/(C_0-C_{\infty})]$ (Figure S2, top). The corresponding rate, $k^{\text{EXP}} = 1.71 \cdot 10^{-6} \text{ s}^{-1}$, was used to model run C. All kinetics data are gathered in Figure S2 (bottom) and were in the range $[10^{-6} - 2 \cdot 10^{-5}] \text{ s}^{-1}$.

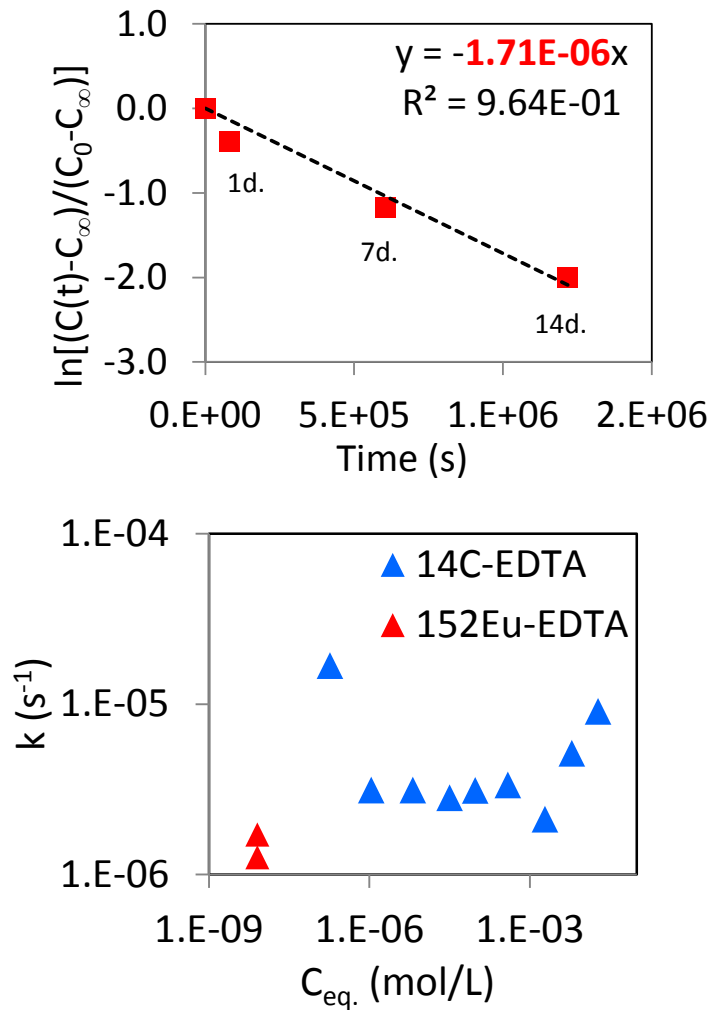


Figure S2. Experimental adsorption kinetics of EDTA complexes on COx clay rock.
 (top) Example of linear regression for $[Eu]_{eq} = 8 \cdot 10^{-9} \text{ mol L}^{-1}$.
 (bottom) Experimental adsorption rates as a function of concentration of adsorbates.

Effect of kinetics on through-diffusion modelling

The effect of slow reversible adsorption kinetics was modelled using semi-analytical solutions provided for through-diffusion cells by Moridis (1998). The adsorption rate for run C was supposed equal to the value measured by batch experiments: $k = 1.71 \cdot 10^{-6} \text{ s}^{-1}$. The best fit was obtained with values $D_e = 1.74 \cdot 10^{-12} \text{ m}^2 \cdot \text{s}^{-1}$ and $K_d = 2.08 \text{ L} \cdot \text{kg}^{-1}$ is presented in figure S3. This modelling highlights two results. Firstly, an early rise of the downstream flux before 70 days may be explained by slow adsorption. Secondly, such adsorption kinetic fail to explain the main difference between R_d measured in batch experiments and K_d adjusted from diffusion experiments.

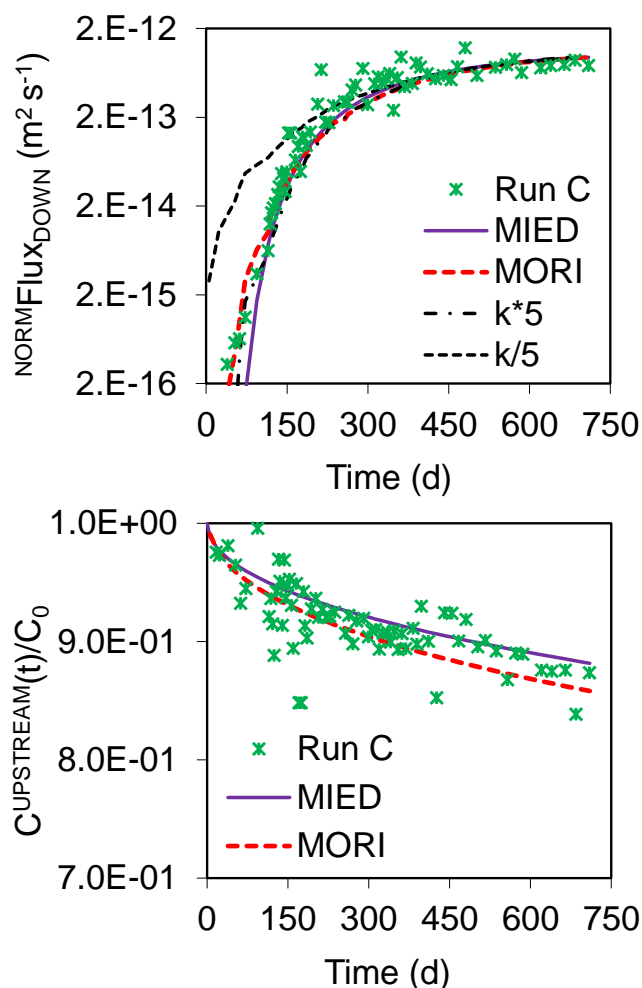


Figure S3. Modelling of downstream flux (top) and upstream concentration (bottom) with two models: MIED and MORI respectively without and with taking into account adsorption kinetics. Adjusted parameters are $(D_e, K_d) = (1.5 \cdot 10^{-12}, 1.8)$ and $(1.7 \cdot 10^{-12} \text{ m}^2 \text{ s}^{-1}, 2.1 \text{ L kg}^{-1})$ for MIED and MORI respectively. Dark curves represent effect of adsorption rates five times higher or five times lower than the experimental value: $k = 1.71 \cdot 10^{-6} \text{ s}^{-1}$.

Bibliography:

Moridis, G.J., 1998. A Set of Semianalytical Solutions for Parameter Estimation In Diffusion Cell Experiments. Sci. New-York.

Wu, S.L., Horrocks, W.D., 1996. General Method for the Determination of Stability Constants of Lanthanide Ion Chelates by Ligand-Ligand Competition: Laser-Excited Eu^{3+} Luminescence Excitation Spectroscopy. Anal. Chem. 394–401.